sciendo

POLISH MARITIME RESEARCH 1 (113) 2022 Vol. 29; pp. 97-107
10.2478/pomr-2022-0010

PREDICTION OF WELD DEFORMATIONS BY NUMERICAL METHODS - REVIEW

Janusz Kozak*
Gdańsk University of Technology, Poland
* Corresponding author: *kozak@pg.edu.pl (J.Kozak)*

ABSTRACT

The welding process is the basic technique of joining in the shipbuilding industry. This method generates welding distortions that cause a lot of problems during the manufacturing process due to both the time and cost of straightening as well as their influence on later stages of production. Proper preparation of welding processes plays a growing role in the shipbuilding industry and the development of calculating tools is being observed. The paper presents a review and critical analysis of numerical methods for the assessment of welding distortion.

Keywords: welding distortion; shipbuilding welding; numerical simulation

INTRODUCTION

During the manufacturing of metal ship hulls, joints of structural elements are generally made using welding techniques. As a result of these processes, complex forms of deformations can occur. In most cases, it is an unexpected effect that strongly influences the quality of the product, as well as the next steps of assembly. Deformations which exceed allowable values may cause problems in assembling the hull's sections or even make the operation completely unfeasible. Excessive deformations observed especially on thin parts of the ship like the sides of the superstructure or side shell plating, which exceed permissible limits, must be removed by straightening, or in extremely unfavourable cases a new structure has to be produced, which extends the manufacturing time and raises its cost. It is evident that the quality of the structural design may to a large extent depend on the susceptibility of the structure to deformation during the production processes. Therefore proper planning in the structural design stage, rational planning of the manufacturing process and then adequate prevention during the fabrication stage has to be undertaken in order to minimise the expected welding deformations. From this point of view, the use of every possible tool should be considered.

WELDING DEFORMATIONS

Welding deformations are defined as changes of the size and shape of structural components, as a result of the thermal cycle during the welding process [1] resulting from the synergy of two actions: solidification contraction of the liquid metal and the plastic deformations of the material close to the weld area during the heating process. The shrinkage forces depend on the type of weld, its size, edges preparation and the welding technique applied. Looking at forms of deformation, one can distinguish:

- Transverse shrinkage – by uneven distribution of the temperature, changing in both weld directions. This causes different shrinkage of both the weld and the heat-affected zone (HAZ). The removal of such deformations is practically impossible.
- Longitudinal – its value is proportional to the energy of the welding arc and inversely proportional to the transverse area of the welded components.
- Torsional – generated by asymmetrical solidification of the material of the weld.
- Angular – caused by asymmetrical shrinkage of the weld and HAZ.

These basic forms can combine and finally result in shortening, bending, torsion or buckling of the structure.

Additionally, for thick welds, shrinkage in the thickness direction can occur [2], as shown in Fig. 1.

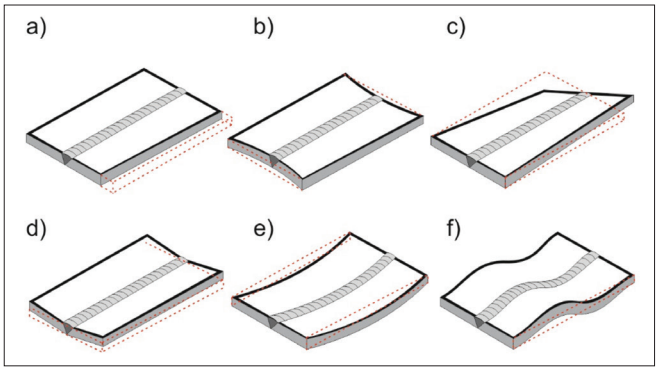

Fig. 1. Forms of post-welding deformations: a) transverse, b) shrinkage, c) twisting, d) angular, e) bending, f) buckling

EMPIRICAL FORMULAE FOR PREDICTION OF POST-WELDING SHRINKAGE

The baseline for calculating the longitudinal deformation of the weld is the formula proposed by Okerblom in 1955, as follows [3]:

$$\varepsilon_L = \frac{\delta_L}{L} = 0{,}335\,\frac{q \cdot \alpha}{A \cdot v_w \cdot c \cdot \rho} \tag{1}$$

where:

δ_L – change of length of weld [mm];
L – initial length of weld [mm];
q – power of heat source [W]; α – thermal expansion coefficient of material $[\frac{1}{K}]$;
A – cross-section area $[mm^2]$;
v_w – velocity of welding process $[\frac{mm}{s}]$;
ρc – volume specific heat of material $[\frac{J}{m^3 \cdot K}]$.

The assumption for such formula is that the whole weld is made in one moment, so it is preferred for short joints, but based upon formula (1), some modifications have been proposed [4], [5], [6], [7], [8], [9], [10].

Another quick way of calculating deformations can be the use of monographs generated from experimental results data. An exemplary diagram for the assessment of the angular distortion of a butt weld joint depending on the geometry and weld parameters is presented in Fig. 2 [11], [12], [13].

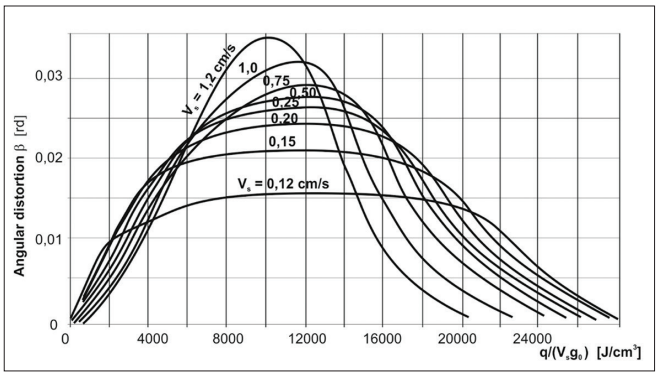

Fig. 2. Diagram for assessment of angular distortion for butt weld joint depending on geometry and weld parameters [11]

NUMERICAL MODELLING

The rapid development of computers, with their increasing capacity and speed, has made it possible to use numerical tools for solving problems of welding deformations. However, precise analysis needs computers with substantial calculation capacity, so the search is on for methods and models that offer a compromise between high accuracy and a reasonable calculation time.

Among others, the Finite Elements Method (FEM) is one of the most popular tools for the numerical solution of engineering problems. Due to the already implemented formulae, such methods give the possibility of reliable modelling of complex processes.

Due to the abovementioned conjugation of changes in the material properties, proper numerical modelling of the welding process is a major challenge. Some general approaches are presented:

- Transient analysis
- Shrinkage-based analysis
- Local–global analysis.

TRANSIENT ANALYSIS

The method based upon transient analysis is relatively the most sophisticated, taking into account such factors as temperature-related properties of the material, particular characteristics of the heat source, the size and shape of the welding pool or microstructural changes of the parent material. Due to the non-linear properties of some of the mentioned properties, such analysis is treated as non-linear, time-domain analysis.

Possible strategies for modelling of the process are presented in Fig. 3 [14].

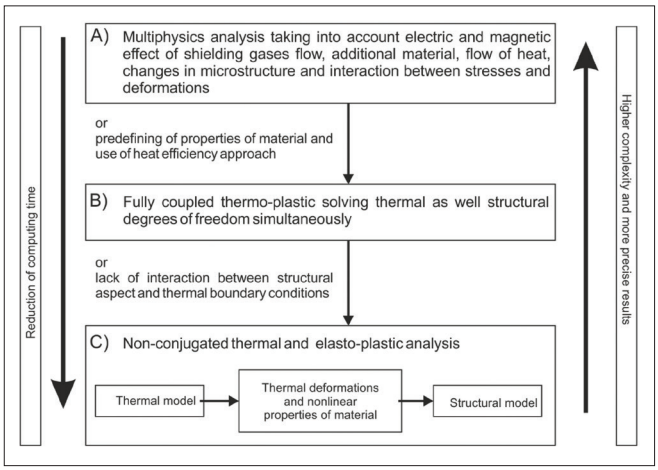

Fig. 3. Strategies for modelling of welding process [14]

For the simplest level of calculations, it is assumed that the mechanical processes that occur during welding have a negligible influence on the thermal properties of the material, whereas the influence of thermal processes on the mechanical properties of the material is crucial. With this assumption, the calculation process can be divided into two steps: thermal

analysis and mechanical analysis, which allow a significant reduction of the calculation time. Thermal analysis in the time domain is performed as the first step of calculation and then the time history of the temperature in each of the nodes of the model is used as the load for structural analysis. This approach is presented in level C in Fig. 3.

Applying this strategy gives some opportunities to influence the model of the analysed geometry. The separation of the two mentioned scopes of calculation makes it possible to increase the density of the mesh by using a combination of two- and three-dimensional mesh elements, and depending on the applied load as either static, quasi-static or time-domain. Each approach has pros and cons in relation to the calculation time, accuracy and computing power required. The relationship between accuracy and the labour demand for the presented approach is shown in Fig. 4.

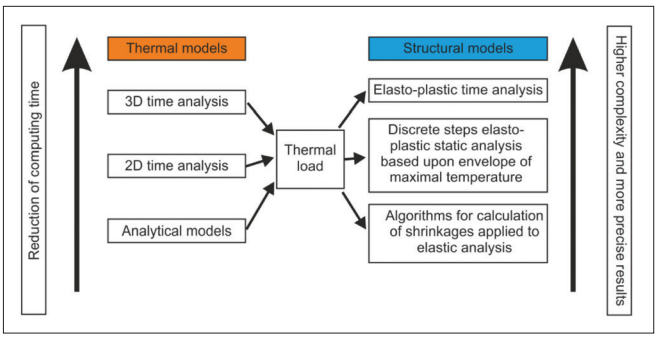

Fig. 4. General approaches for non-coupled calculation [15]

In the process of thermal analysis, independently of the algorithms applied, there are some fundamental problems like the mesh topology, modelling of the material's properties or proper application of the heat source.

Discretisation – mesh topology

Proper design of the mesh is a crucial factor for both the accuracy of calculations and the computing time or computer power required. One should keep in mind that the searched values are calculated only for nodal points, whereas are interpolated on the whole area between nodes. From this point of view, the area close to the weld region has to be meshed in detail by dense elements due to the presence of high temperature gradients close to the welding pool. On the other hand, the number of degrees of freedom, which is related to the number of nodes, strongly influences the time and required power of the calculation. A number of papers present data on the relationship between accuracy and the level of density of the mesh [16] [17] [18].

Proper definition of the characteristics of the heat source as well as the way of applying it is crucial for the accuracy of modelling. Finally, boundary conditions like convection or thermal radiation have to be established. During such analysis, the technique of element birth/death is used to take proper account of the way of laying on additional material.

When the thermal loads for each nodal point are recorded for a given moment of time, mechanical modelling can be done as quasi-static or time-dependent. For these types of modelling, changes of the properties of the material in relation to the temperature are taken into account, including changes in the plasticity of the material. This type of analysis is named "thermo-elastic-plastic" (TEP) [19]. At this stage of calculation, the element birth/death technique is used. A scheme of the sequence for carrying out the TEP simulation is presented in Fig. 5.

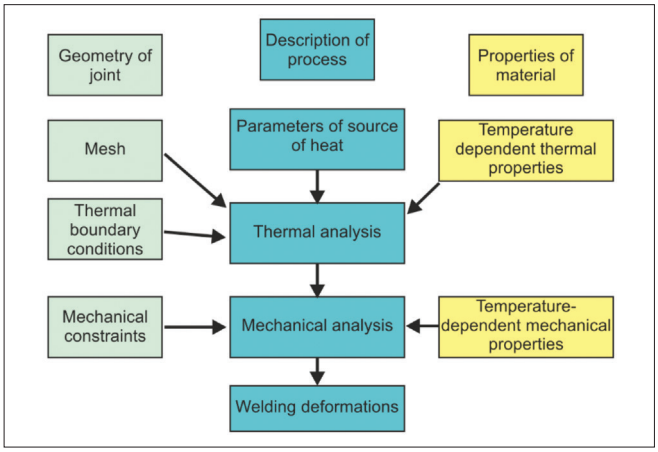

Fig. 5. Sequence for carrying out TEP simulation [19]

Modelling of material properties during welding

The mechanical characteristics of steel strongly depend upon its grade [20], [21]. Particular data especially on the relationship of the mechanical properties and the temperature are rarely available. The most credible source of data are the laboratory test results carried out on specimens of the analysed material but it requires attempt to laboratory infrastructure; however, there are some data implemented in commercial software like JMat Pro® [22], [23]. Due to difficulties in obtaining exact data on a particular material, a deviation of data in the range of ±10% regarding the true value is considered, which does not influence the results of the modelling [16].

Among the mechanical properties for the modelling of mechanical processes are: yield point R_e, ultimate strength R_m, Young's modulus E and thermal expansion coefficient α, whereas the thermal properties include: specific heat C, heat conductivity k and coefficient of convection η. The main problem in applying these parameters for modelling is that all of them change in a non-linear way depending upon the temperature. As an example, the value of the thermal expansion coefficient for shipbuilding steel as a function of temperature is presented in Fig. 6 [15]. Besides the change in its value, the observed data differ between the heating and cooling action.

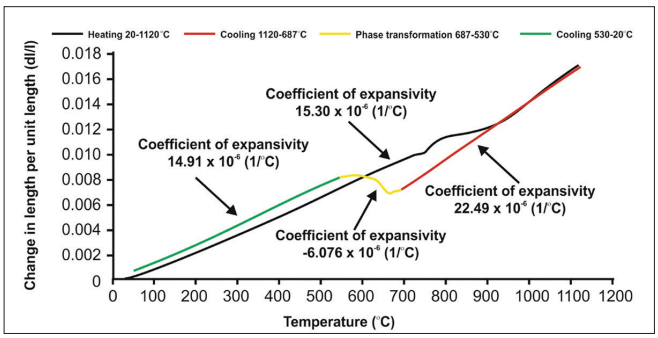

Fig. 6. Coefficient of thermal expansivity for shipbuilding structural steel DH36 [15]

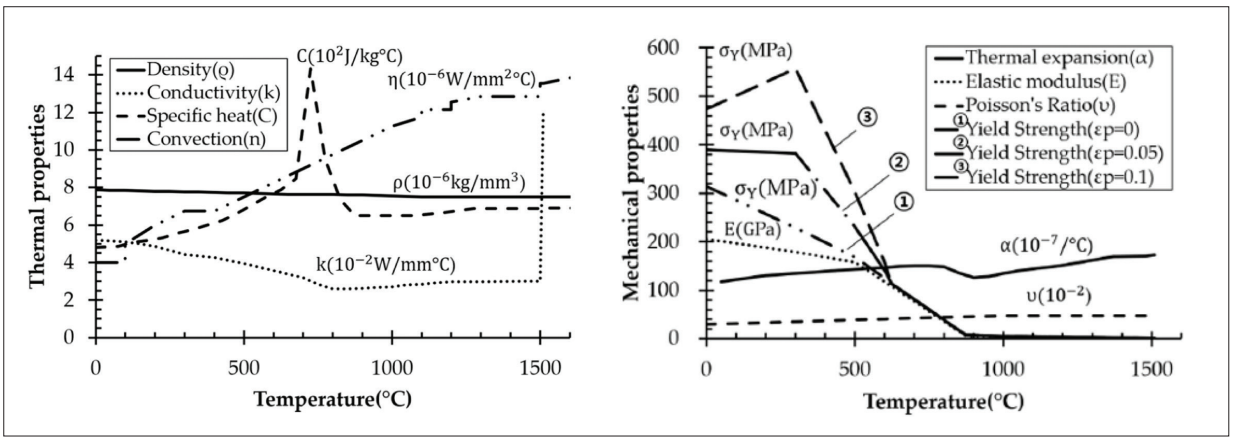

Fig. 7. Properties of shipbuilding structural steel AH32 for welding process temperature range [24]

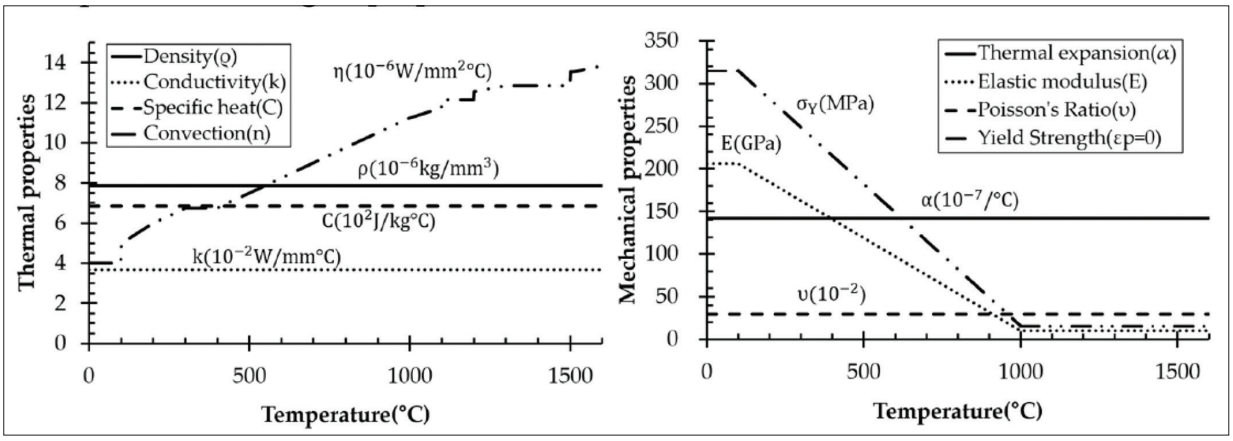

Fig. 8. Example of simplification of properties of material [24]

Looking at the changes of properties for another shipbuilding steel (Fig. 7), the same problems (variation with temperature, non-linearity) can be observed [24].

Taking into account the presented characteristics, one can assume that for modelling of the welding process it is necessary to approximate the material characteristics by line segments representing average values for a given interval [15]. An example of such approach is presented in Fig. 8 [24].

Application of heat sources for modelling of welding processes

Welding needs heat energy for melting of the material to allow joining. An important factor in numerical modelling of the welding process is a proper representation of all the important features of the applied source of welding heat. Each welding method presents a specific density distribution of the heat energy. The laser or electron beam method presents narrow and deep penetration with a narrow HAZ, whereas the arc or plasma welding method shows rather a medium energy density as presented in Fig. 9.

This variety of shapes and parameters has a strong influence on the accuracy of modelling. Measurement or checking of the welding pool and its closest surroundings is difficult, so it is difficult to obtain such data with error less than 5% [26]. The variable characteristics of the wire material as well as the shielding gas also give rise to difficulties in modelling.

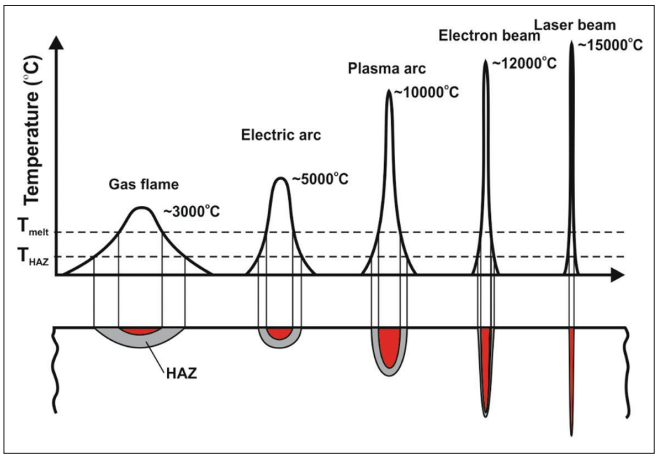

Fig. 9. Size of HAZ and depth of penetration for different welding methods [25]

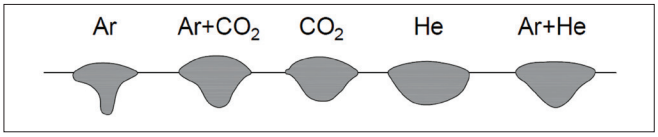

Fig. 10. Shape of cross-section of weld depending upon shielding gas [25]

Examples of the shape of the weld depending upon the shielding gas applied are presented in Fig. 10. Information on the shape of the weld can also play a role in the modelling process.

The next important factor influencing on the process of modelling is purpose of calculation: for assessing the hot cracking process, an exact model of the welding pool is necessary, whereas for modelling of the post-welding strain and stresses, a representation of the temperature field in the joint is sufficient [26].

There are some proposals for modelling of the heat source.

One of these is the circle shaped surface stream of power, in which the power density is described by a Gaussian distribution:

$$q(r) = q(0)e^{-Cr^2} \tag{2}$$

where

$q(r)$ – stream of power on radius r [W/m^2];
$q(0)$ – maximum power in the middle of the source [W/m^2];
C – coefficient of width of distribution [m^{-2}];
r – radial coordinate [m].

The influence of the C parameter on the distribution is illustrated in Fig. 11.

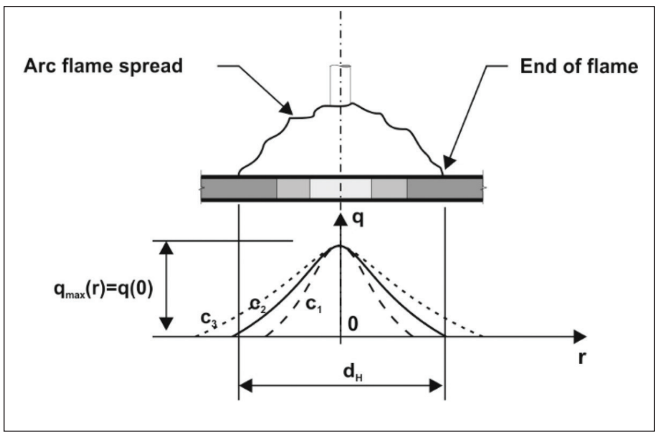

Fig. 11. Model of disc source of heat [26]

For a movable heat source, the presented model is expanded depending on the time and location domain:

$$q(x, y, t) = \frac{3Q}{\pi c^2} e^{-\frac{3x^2}{c^2}} e^{-3[x+v(\tau-t)]^2/c^2} \tag{3}$$

where:

x, y – coordinates of location of source [m];
t – time [s];
Q – power of heat source [W];
c – parameter of shape of curve [m];
τ – location of heat source for t = 0.

This model is good for a small depth of penetration for a relatively low power heat source.

The next model, which takes into account a deep penetration, assumes an ellipsoidal power distribution, with the ellipsoid defined by half the length of the axis a, b, c in x, y , z direction respectively. This model, for a heat source moving in the x-axis direction, describes the locally located specific power density by formula (4):

$$q(x,y,t) = \frac{6\sqrt{3}Q}{abc\pi\sqrt{\pi}} e^{-3[x+v(\tau-t)]^2/a^2} e^{-3y^2/b^2} e^{-3z^2/c^2} \; [W/m^3] \tag{4}$$

where the parameters are the same as for formula (3).

More precise than formula (4) is the model of a double ellipsoid proposed by Goldak [26], which reflects the changed energy distribution down to the welding track. For this reason, the ellipsoid is split into two regions, each separately modelling the power distribution for the front f_f as well as rear part of the weld f_r respectively. X- size for each part: a_f and a_r is defined and the whole energy stream is divided for each part by the fractional coefficients f_f and f_r . The shape of the such defined heat source is presented in Fig. 12, where green colour depicts the front part and blue is the rear part of the ellipsoid. Red indicates the area common to both parts [15]. It is possible to increase the accuracy of this representation by dividing the ellipsoid into more parts.

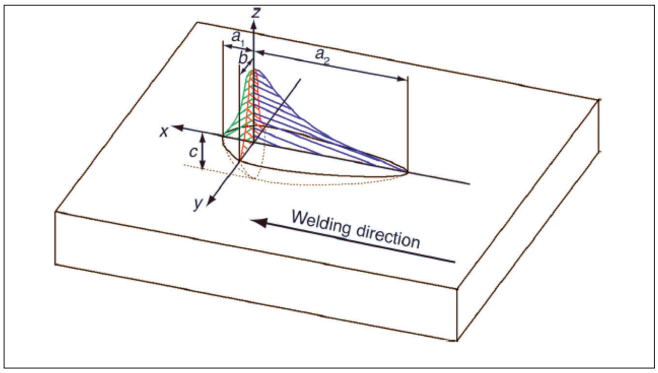

Fig. 12. Model of double ellipsoid [15]

This model gives a good representation of the MIG, MAG or TIG processes and has been verified for a number of cases. Rong et al. applied this model to simulate the joining of 10 mm plates for a MAG process using TEP analysis [27]. The authors observed good agreement between the numerical and experimental test results. The temperature distribution was almost identical for both types of experiment. Long et al. used this approach for modelling the butt welding of 2.5 and 3 mm thick plates [28] to study the influence of the parameters in Goldak's model on the volume of melted material and the size of the HAZ. They concluded that proper calibration of the parameters of the model is possible through feedback with the size of the weld and HAZ. The angular distortions calculated and measured empirically presented a similar form, but the numerical results were almost two times less than the experimental ones and this discrepancy increased with the increasing speed of welding (Fig. 13).

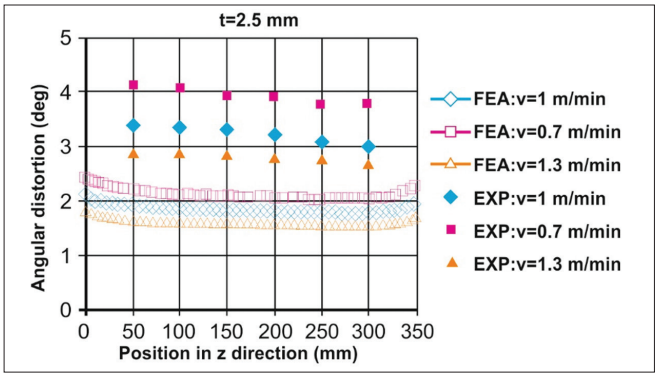

Fig. 13. Angular distortion for different speed of welding [28]

Another example of the utilisation of the double ellipsoid model was presented by Knoedel et al. [29] for the assessment of post-welding stresses. A huge part of their paper was focused on the way of selecting the model's parameters and its influence on the time-related distribution of the temperature. These parameters were calibrated based upon the measured temperature during laboratory experiments, with satisfactory results.

Silva et al. [30] presented a methodology for determining the stream of heat for TIG butt welding of thin plates. They proposed a reversed approach based on experimental data supported by a three-dimensional model based on the coupling gradients method, calibrated by experimental data. The results of the elaborated model compared well with the experimental data.

Deng et al. [19] presented the application of a half-ellipsoidal model with constant heat distribution, where the heat source is defined as:

$$q = \frac{3\eta UI}{2\pi abc} \tag{5}$$

where:
U voltage of arc, I – current, η efficiency of arc, a,b and c – geometrical parameters of the proposed model, calibrated to give the best representation of the melted area.

The influence of different characteristics of the heat source was presented by Heinze et al. in their study of the butt welding of 5 mm plate [31]. Two models of the welding arc were combined: to the face of the weld a Gaussian distributed model was applied, whereas for the welding toe the shallow model proposed by Goldak was used. The size and shape of the welding pool was analysed for four different sets of parameters. Visualisations of the welding pool obtained during numerical simulations were compared with the real measured case (Fig. 14), and the analytically obtained pictures for the two cases are presented in Fig. 15.

An important conclusion was that such a simulation is very sensitive to even small changes of parameters, such as the material's conductivity coefficient, the energy introduced or the shape of isotherm at 1440°C, which represents the shape of the welding pool. Fig. 16 presents a comparison of the numerical versus experimental angular deformations.

In the case of processes using a high power density like laser welding, a suitable model of the power distribution can be a three-dimensional version of the surface stream of the heat with one more factor added – the depth of penetration. A similar and sometimes more accurate model of the heat source is in the form of a truncated cone [26], [32]:

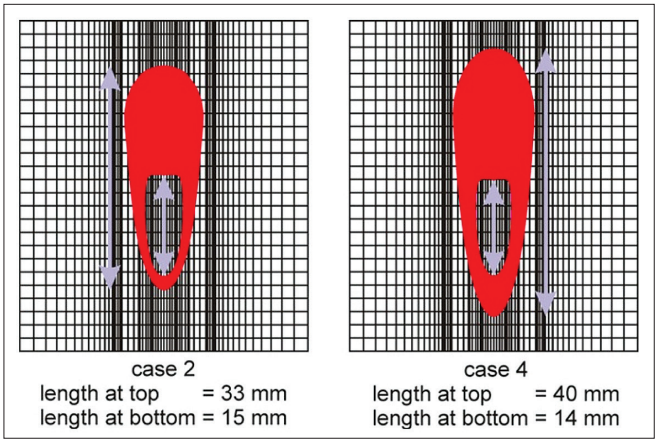

Fig. 15. Comparison of weld pool length at top and bottom of the plate due to the different thermal conductivity applied (in quasi-steady state) [31]

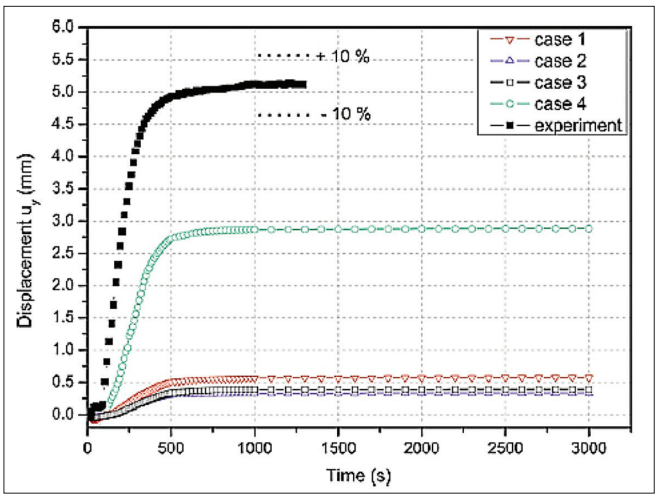

Fig. 16. Comparison of calculated and experimental transient displacement in y-direction [31]

$$q_v(x,y,z) = \frac{9\eta\phi e^3}{\pi(e^3-1)} \cdot \frac{1}{(z_e-z_i)(r_e^2+r_e r_i+r_i^2)} exp\,\frac{3(x^2+y^2)}{r_0^2(z)} \tag{6}$$

where: $r_0(z) = r_e + \frac{r_i - r_e}{z_i - z_e}(z - z_e)$,

re – radius of cone base on surface of material,
r_i – radius of second cone base,
$(z_e - z_i)$ – height of body,
ϕ, η – power and output of power of heat respectively.

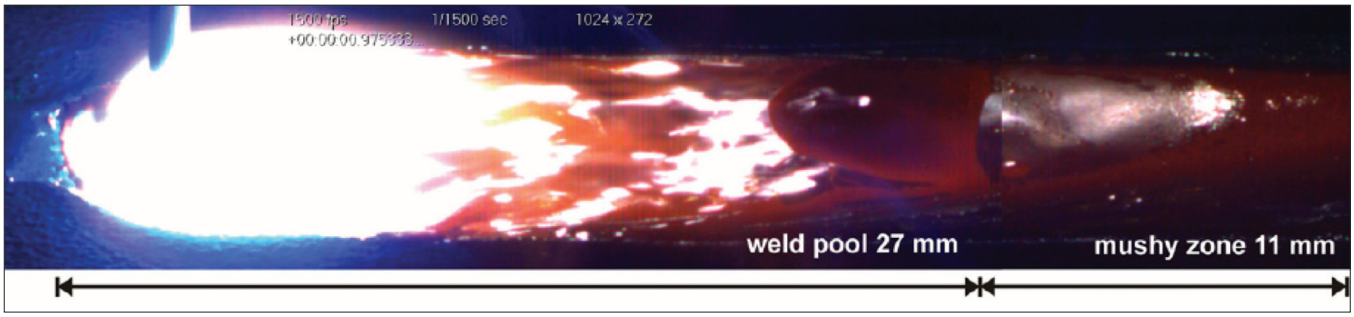

Fig. 14. Experimental image of weld pool during welding, total weld pool length is approx. 38 mm, GMAW, net heat input = 1 kJ/mm [31]

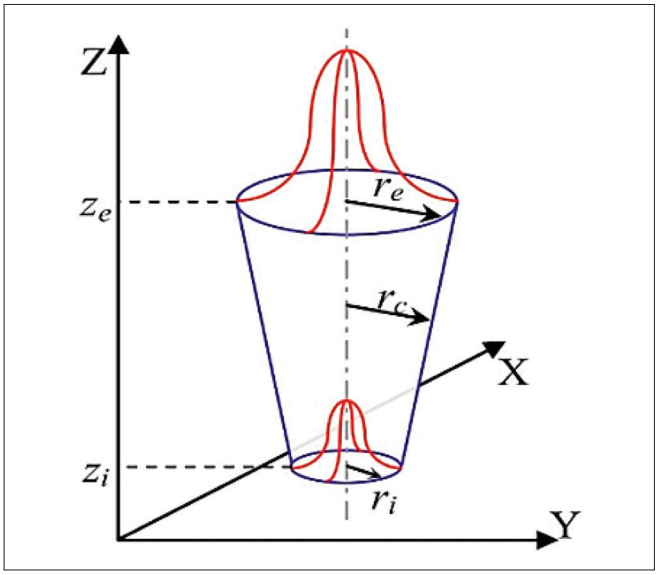

Fig. 17. Truncated cone models with normal power distribution [32]

Fig. 17 presents a visualisation of the described model.

However, practical implementation of such a model shows that it is not adequate for every grade of steel.

Akella et al. have studied models of heat sources fitted to the modelling of laser beam welding [33]. Different models were analysed based upon the horizontal distribution of the stream of heat and the sizes of HAZ generated. They modified the model of the heat source by combining a normal Gaussian with a truncated cone (frustrum) distribution. The latter represents the character of the process well, whereas the normal distribution makes it possible to control the efficiency of the process. Comparison of the characteristics of the new model in relation to its components is presented in Fig. 18.

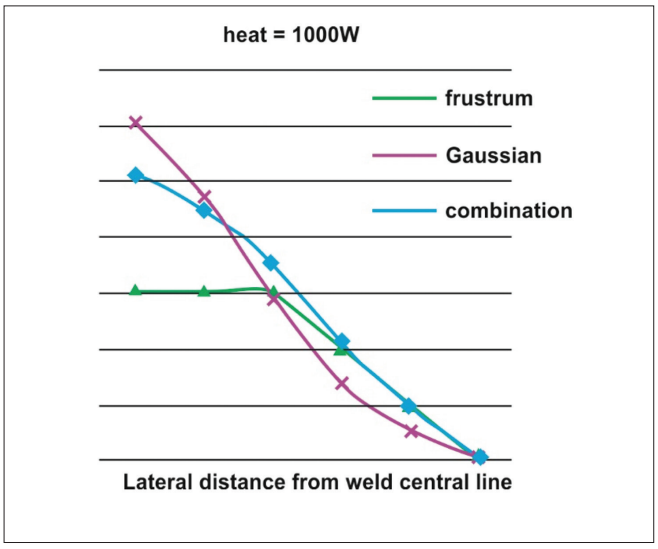

Fig. 18. Effect of combination of two sources of heat for laser welding [33]

Zhan et al. [34] also investigated the model of a heat source suitable for laser welding process modelling. They proposed an hourglass model of the heat source. Comparison of the numerical and experimental results of the laser welding of 6 mm plates of 1060 steel shows good agreement (Fig. 19).

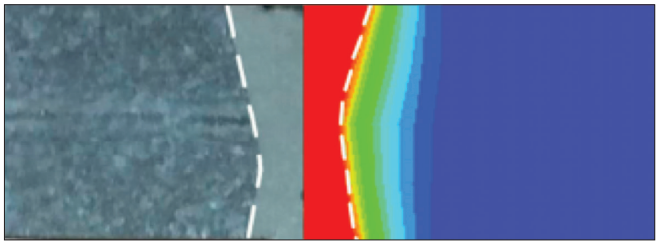

Fig. 19. Cross-section of weld for 1060 steel: experimental versus numerical [34]

The methods presented above focused on the most reliable modelling of the welding heat source by searching for proper parameters for its description. In shipbuilding, the use of such accurate methods by engineers is very difficult for practical implementation due to the sizes of the analysed structures. Chiumenti et al. state that exact representation of the source of welding heat makes sense only for research itself [35]. For this reason, some proposals have been made for simplified modelling to reduce both the pre-processing and computing time.

Peric et al. carried out a simulation of a MAG fillet welding process for 10 mm plates using the Constant Heat Flux method (CHF), applied to elements representing additional material [36]. The weld was divided into blocks which were activated or deactivated at a given moment of time of the process. The quantum of heat for one such step of analysis is described as (7):

$$Q = \frac{\eta UI}{V_H}\left[\frac{J}{m^3 s}\right] \tag{7}$$

where:

η – heat efficiency of process,

V_H – volume of activated block of weld.

Here the geometrical parameters of the welding pool are not taken into account. The calculation results were compared with the record of the thermo-vision camera and it was deduced that the thus defined heat source gives an underestimation of the results of the temperature profiles, but there was good agreement (experimental and numerical) on the angular deformation of the joint.

Barsoum et al. applied a modified CHF method to assess the residual stresses and fatigue life of welded structures [37]. It was proposed to split the total stream of heat into two components: surface and volume [22]:

$$Q_{total} = Q_{surface} + Q_{volume} \tag{8}$$

and the relation $Q_{surface}/Q_{volume}$ can more precisely represent the of area of both the melted metal and the HAZ. Calibration of those relations can be performed in two ways: if the experimentally measured temperature distribution is available, the calibration process tends to reach of the similarity in modelling; if such data are not available, assessment is done based upon the analysis of the temperature in additional material (checking whether all the volume has been melted) as well as on checking of the HAZ size.

Chiumenti et al. related the stream of heat to the speed of delivery of the welding wire [35]:

$$Q = \frac{\eta V I}{V_{feed}} \tag{9}$$

$$V_{feed} = \frac{\pi}{4}\varphi^2_{feed} \cdot v_{eed} \cdot \Delta t \tag{10}$$

where:

V_{feed}, φ_{feed} and v_{feed} – volume diameter and speed of delivery of welding wire,

Δt – time interval.

The calculated angular distortion was in good agreement with the real values.

Capriccioli et al. studied the influence of the method of application of heat on deformations during multi-run welding of thick plates [16]. Two methods: CHF with a constant power output [W] and CHF with a constant power density $\left[\frac{W}{m^3}\right]$, were analysed. During the welding of the thick plates, a number of weld layers with different cross-sections occur (Fig. 20). This causes complications in the case of applying the first-mentioned method, with the possible influence of the size of the block on the temperature, as bigger blocks have a lower maximal temperature. Application of the second mentioned approach resulted in the reverse effect.

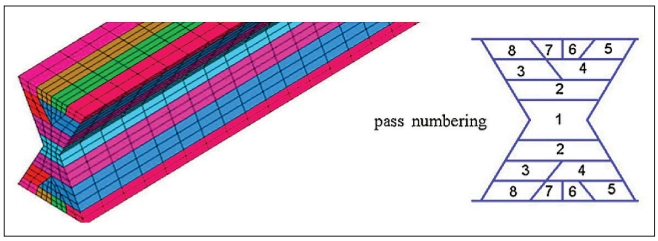

Fig. 20. Differentiation of size for particular layers [16]

Another way of simplifying the TEP analysis was presented by Seles et al. [38]. The authors compared the efficiency of the CHF method with their own elaborated "Prescribed Weld Temperature Method" (PWT). Contrary to TEP, they proposed instead to apply evenly distributed heat power $\left[\frac{W}{m^3}\right]$ to the activated block, only activating blocks with a given temperature [°C]. Two variants of mechanical analysis were performed: for one case (M1 in Fig. 21) the weld was divided into parts and the technique of activating/deactivating the element was used; for the second one (M2 in Fig. 21) the weld was modelled by the simultaneous weld deposition method (without the activating/deactivating technique). Analysis was performed for two types of joints: the butt joint of 6 mm plates and fillet joints of 10 mm plates. The results were promising – the temperature distribution in the plates was similar for both approaches, but application of the PWT method resulted in a significant reduction of the computing time (Fig. 21). Fig. 22 presents the angular distortions, which were almost the same

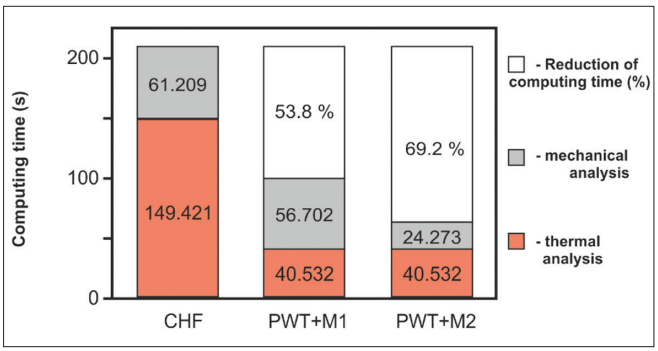

Fig. 21. Comparison of computing time for different methods [38]

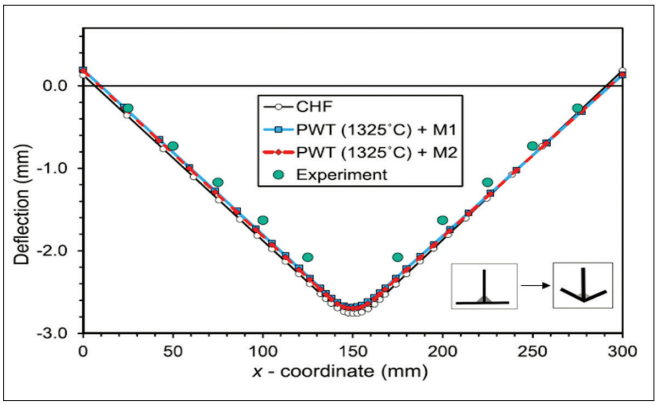

Fig. 22. Comparison of angular distortions of T-joint calculated for different methods [38]

for both variants of calculation. The PWT approach was tested also by Capriccioli [16].

METHODS FOR REDUCTION OF COMPUTING TIME

The complexity and non-linearity of the processes of simulating welding processes result in long calculation times, especially if full TEP analysis is carried out. For the reduction of such an obstacle, some proposals have made to mix both 2D and 3D elements in one TEP model due to the fact that non-linear description of the behaviour of the material plays an important role only close to the weld. This approach significantly reduces the number of nodes [27]. Peric et al. applied such an approach and reached a time reduction of up to 42% [36], [39].

Another method for time reduction is pass-lumping, by joining some passes together to give the possibility of simultaneous laying. Such a method for butt welding of thick plate is presented in Fig. 23, where different levels of simplification are shown. Klassen et al. also tested this approach and concluded that the crucial factor for accuracy of the results

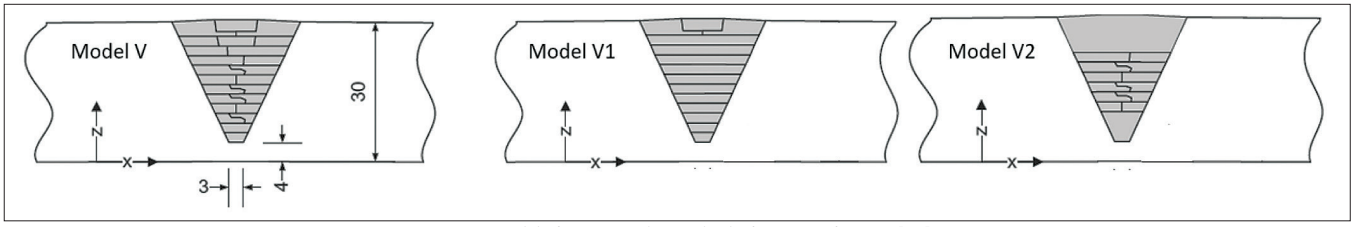

Fig. 23. Models for testing the method of joining of passes [40]

is the degree of simplification [40]. Model V1 has almost twice lower results compared to the non-simplified model V, whereas the results for model V2 were similar to those of model V.

Yang et al. presented a study for modelling welding deformations for shipyard processes, analysing thin walls with mock-up sizes of 5 x 2.5 m [41]. The pass-lumping approach made it possible to reduce the weld layers from over 300 to 86. The results were compared with the effect of simulation with a mobile heat source and laying each pass separately, as well as with measurement on a real mock-up structure. The results were compared for 13 points due to the complexity of the object. The results of the numerical analysis were comparable but not quite in agreement with the measurements. This approach was used also by other authors [22], [42].

Another proposed method for reducing the computing time is by subdivision of the analysed structure into low-level components (substructures). For this method, the region close to the weld is defined with a non-linear description of its properties, whereas regions modelling the rest of the structure are described in simplified way as behaving linearly. It is assumed that plastic deformations in the steel take place at temperatures above 125°C, which can be one of the criteria for subdivision. For this reason, it is necessary to create two models of the material for each substructure. Visualisation of the meshing is presented in Fig. 24.

Guiaro et al. developed an algorithm for performing a simulation based upon substructures [43]. Barsoum et al. presented the application of this method for massive beam geometry and found about a 20% reduction of computing time [44]. Zhu et al. showed an example of applying this

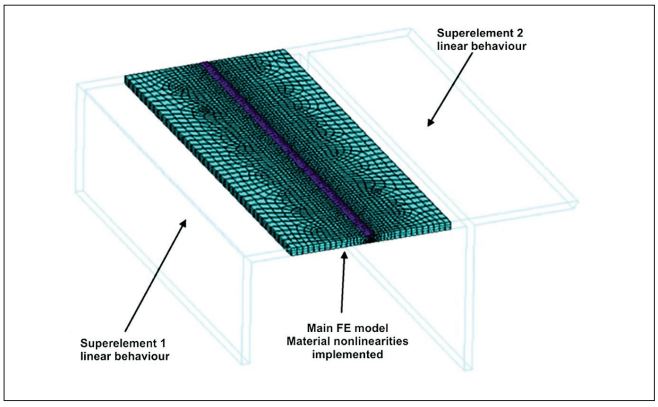

Fig. 24. Mechanical sub-structuring process [43]

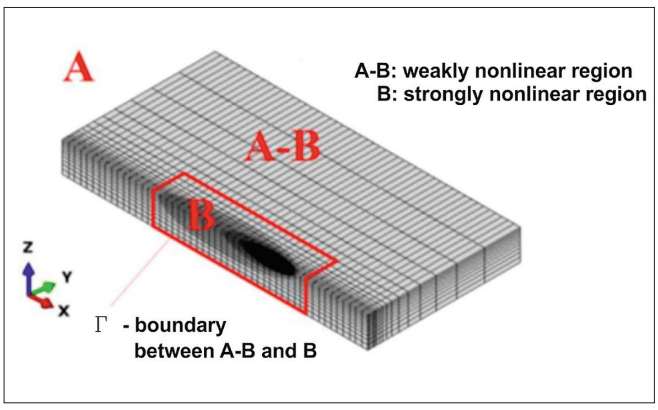

Fig. 25. Concept of iterative substructure method (ISM) [45]

methodology for small structures but did not observe a significant reduction of the calculation time for the analysed configuration [23]. Huang et al. proposed such an approach in their Iterative Substructuring Method – ISM [45]. Based upon Murakawa et al.'s [46] works, they divided the analysed geometry into regions: with strong non-linearity (B) and less non-linear (A-B) (Fig. 25).

Contrary to the classical approach, here the boundary of the strongly non-linear area is fluent and changes during the calculation process based on the assessment of the size of the area with a high temperature gradient, which changes with movement of the welding pool. Calculations for both areas are conjugated. Region (B) is small so the results can be calculated in a relatively short time and compared with the results for the (A-B) area. If the results are not close, calculation of region (B) is the starting point for a new calculation process for the (A-B) area. This approach allows a reduction of the computing time by up to 75%, with accuracy practically at the same level as for the full calculation process by the TEP approach.

Similar research was carried out by Rong et al. [47] for modelling the welding process for big shipbuilding panels. To reduce the computing time, the parallel computing method (PCM) was applied, combining a CPU and GPU. This approach was also applied by Wang et al. for the assessment of a container ship structure [48]. An example of the application of the PCM approach can be found in [49].

SUMMARY

Methods for numerical modelling of welding processes are presented below.

- Models of the heat source for utilisation in the calculation process have been presented and discussed.
- Approaches to representing the material properties in relation to the temperature of the welding process were described in the literature review.
- Three approaches to simulation of the welding processes were described. The pros and cons of the particular processes were discussed.
- Criteria for proper selection of the given approach were discussed, focusing on the purpose of the calculation, required accuracy, available power of the computer system or expected computing time.
- Thermomechanical non-linear time domain analysis is suitable for a small, less complicated geometry or when highly accurate calculation is required. This approach makes it possible to analyse the time history of the process and can be an introductory step for further analysis.
- Simplified analysis is more suitable for large structures with complicated geometry like panel sections or blocks in the shipbuilding industry. The use of such method is easy, pre-processing is not too complicated, the computing time is relatively short and the accuracy of the results is acceptable for the purposes of engineering calculations, but it gives only "final" information without the history of evolution.
- A method joining two mentioned approaches is the

local-global approach which delivers satisfactory results within a reasonable pre- and processing time.

REFERENCES

1. L.M. Gourd, *Principles of Welding Technology*, The Welding Institute, London, 1995.
2. R. Hetnarski, Ed., *Encyclopedia of Thermal Stresses*, Springer Link, 2014.
3. N. Okerblom, Schweissspannungen in Metallkonstruktionen, Halle: Veb Carl Marhold Verlag, 1956.
4. G. Verhaeghe, *Predictive Formulae for Weld Distortion: A Critical Review*, Abington Publishing, 1999, ISBN 185573 444 3., 1999.
5. C. G. Soares and T. A. Santos, Eds., *Maritime Technology and Engineering*, vol. 1, Lisbon: CRC Press, 2014.
6. M. Watanabe and K. Satoh, "Effect of welding conditions on the shrinkage and distortion in welded structures", *Welding Journal*, 1961.
7. V. Murugan and V. Gunaraj, "Effects of Process Parameters on Angular Distortion of Gas Metal Arc Welded Structural Steel Plates", *Welding Journal*, 2005.
8. R. W. O'Brien, "Predicting weld distortion in the design of automotive components", Durham University, Durham, 2007.
9. K. Sun, Y. Shi, Y. Hu and B. Liao, "Microstructure Evolution and Mechanical Properties of Underwater Dry Welded Metal of High Strength Steel Q690E under Different Water Depths", *Polish Maritime Research*, vol. 27, no. 4, 2020.
10. H. Li, S. Liu, Q. Ma, P. Wang, D Liu and Q. Zhu, "Investigation of Process Stability and Weld Quality of Underwater Wet Flux-Cored Arc Welding of Low-Alloy High-Strength Steel with Oxy-Rutile Wire", *Polish Maritime Research*, vol. 28, no. 3, 2021.
11. J. Kozak and J. Kowalski, "Problems of determination of welding angular distortions of T-fillet joints in ship hull structures", *Polish Maritime Research*, vol. 22, no. 2(86), pp. 79-85, 2015.
12. J. Kozak and J. Kowalski, "The Influence of Manufacturing Oversizing on Postwelding Distortions of the Fillet Welded Joint", *Polish Maritime Research*, vol. 22, no. 4(88), pp. 59-63, 2015.
13. M. Maternowski, Application of numerical methods for prediction of weld deformations of thin plates butt welded as well as laboratory verification of the results, Diploma thesis, Gdansk University of Technology, Faculty of Ocean Engineering and Ship Technology, (in Polish), 2021.
14. J. Wang, H. Zhao, J. Zou, H. Zhou, Z. Wu and S. Du, "Welding distortion prediction with elastic FE analysis and mitigation practice in fabrication of cantilever beam component of jack-up drilling rig", *Ocean Engineering*, 2017.
15. T. Gray, Ed., *Control of welding distortion in thin-plate fabrication*, Cambridge, Woodhead Publishing Limited, 2014.
16. A. Capriccioli and P. Frosi, "Multipurpose ANSYS FE procedure for welding processes simulation", *Fusion Engineering and Design*, no. 84, 2009.
17. S. Joshi, J. Hildebrand, A. S. Aloraier and T. Rabczuk, "Characterization of material properties and heat source parameters in welding simulation of two overlapping beads on a substrate plate", *Computational Materials Science*, no. 69, 2013.
18. C. Heinze, C. Schwenk and M. Rethmeier, "Influences of mesh density and transformation behavior on the result quality of numerical calculation of welding induced distortion", *Simulation Modelling Practice and Theory*, no. 19, 2011.
19. D. Deng, Y. Zhou, T. Bi and X. Liu, "Experimental and numerical investigations of welding distortion induced by CO2 gas arc welding in thin-plate bead-on joints", *Materials and Design*, no. 52, 2013.
20. A. A. Bhatti, Z. Barsoum, H. Murakawa and I. Barsoum, "Influence of thermo-mechanical material properties of different steel grades on welding residual stresses and angular distortion," *Materials and Design*, no. 65, 2015.
21. D. Deng, "FEM prediction of welding residual stress and distortion in carbon steel considering phase transformation effects", *Materials and Design*, 2009.
22. Z. Barsoum, A. A. Bhatti and S. Balawi, "Accuracy of computational welding mechanics methods for estimation of angular distortion and residual stresses", in *1st International Conference on Structural Integrity*, Kalpakkam, 2014.
23. J. Zhu, M. Khurshid and Z. Barsoum, "Accuracy of computational welding mechanics methods for estimation of angular distortion and residual stresses", *Welding in the World*, no. 63, 2019.
24. S. C. Park, H. S. Bang and W. J. Seong, "Effects of Material Properties on Angular Distortion in Wire Arc Additive Manufacturing: Experimental and Computational Analyses", *Materials*, 2020.
25. K. Ferenc, *Welding*, Warszawa: Wydawnictwa Naukowo-Techniczne, 2007 (in Polish).
26. J. A. Goldak and M. Akhlaghi, *Computational Welding Mechanics*, New York: Springer Science+Business Media, 2005.
27. Y. Rong, G. Zhang and Y. Huang, "Study of Welding Distortion and Residual Stress Considering Nonlinear Yield Stress Curves and Multi-constraint Equations", *Journal of Materials Engineering and Performance*, 2016.

28. H. Long, D. Gery, A. Carlier and P. Maropoulos, "Prediction of welding distortion in butt joint of thin plates," *Materials and Design*, 2009.

29. P. Knoedel, S. Gkatzogiannis and T. Ummenhofer, "Practical aspects of welding residual stress simulation", *Journal of Constructional Steel Research*, 2017.

30. S. Silva, L. Vilarinho, A. Scotti, T. H. Ong and G. Guimaraes, "Heat flux determination in the gas tungsten-arc welding process by using a three-dimensional model in inverse heat conduction problem", *High Temperatures–High Pressures*, 2003/2004.

31. C. Heinze, C. Schwenk and M. Rethmeier, "Effect of heat source configuration on the result quality of numerical calculation of welding-induced distortion", *Simulation Modelling Practice and Theory*, 2012.

32. S. Vrtiel and M. Behulova, "Analysis of laser beam welding of the S650MC high strength steel using numerical simulation," in *IOP Conference Series: Materials Science and Engineering*, 2019.

33. S. Akella, H. Vemanaboina and R. K. Buddu, "Heat Flux for Welding Processes: Model for Laser Weld", *Sreyas International Journal of Scientists and Technocrats*, 2016.

34. X. Zhan, G. Mi, Q. Zhang, Y. Wei and W. Ou, "The hourglass-like heat source model and its application for laser beam welding of 6 mm thickness 1060 steel", *International Journal of Advanced Manufacturing Technology*, 2017.

35. M. Chiumenti, M. Cervera, A. Salmi, C. A. Saracibar, N. Dialami and K. Matsui, "Finite element modeling of multi-pass welding and shaped metal deposition processes", *Computer Methods in Applied Mechanics and Engineering*, 2010.

36. M. Peric, Z. Tonkovic, A. Rodic, I. Garasic, I. Boras and S. Svaic, "Numerical analysis and experimental investigation of welding residual stresses and distortions in a T-joint fillet weld", *Materials and Design*, 2014.

37. Z. Barsoum and I. Barsoum, "Residual stress effects on fatigue life of welded structures using LEFM", *Engineering Failure Analysis,* 2009.

38. K. Seles, M. Peric and Z. Tonkovic, "Numerical simulation of a welding process using a prescribed temperature approach", *Journal of Constructional Steel Research*, 2018.

39. M. Peric, D. Stamenkovic and V. Milkovic, "Comparison of Residual Stresses in Butt-Welded Plates Using Software Packages Abaqus and ANSYS", *Scientific Technical Review*, vol. 60, 2010.

40. J. Klassen, T. Nitschke-Pagel and K. Dilger, "Simplified residual stress and distortion calculations of multi-pass welds and their possible influence on result quality", *Welding in the World*, 2019.

41. Y. Yang, F. Brust, Z. Cao, J. Kennedy, X. Chen, Z. Yang and N. Chen, "Lump-Pass Welding Simulation Technology Development for Shipbuilding Applications", in *6th International Trends in Welding Research 2002*, Pine Mountain, USA, 2003.

42. P. Dong, J. Hong and P. Bouchard, "Analysis of residual stresses at weld repairs", *International Journal of Pressure Vessels and Piping*, 2005.

43. J. Guirao, E. Rodriguez, A. Bayon and L. Jones, "Use of a new methodology for prediction of weld distortion and residual stresses using FE simulation applied to ITER vacuum vessel manufacture", *Fusion Engineering and Design*, 2009.

44. [44] Z. Barsoum, A. Bhatti and S. Balawi, "Computational Weld Mechanics – Towards a simplified and cost effective approach for large welded structures", in 1st International Conference on Structural Integrity, Funchal, 2015.

45. H. Huang, N. Ma, T. Hashimoto and H. Murakawa, "Welding Deformation and Residual Stresses in Arc Welded Lap Joints by Modified Iterative Analysis", *Science and Technology of Welding & Joining*, 2015.

46. J. Wang, H. Yuan, N. Ma and H. Murakawa, "Recent research on welding distortion prediction in thin plate fabrication by means of elastic FE computation", *Marine Structures*, 2016.

47. Y. Rong, J. Xu, Y. Huang and G. Zhang, "Review on finite element analysis of welding deformation and residual stress", *Science and Technology of Welding and Joining*, 2018.

48. J. Wang, X. Shi, H. Zhou, Z. Yang and J. Liu, "Dimensional precision controlling on out-of-plane welding distortion of major structures in fabrication of ultra large container ship with 20000TEU", *Ocean Engineering*, 2020.

49. N. Ma, "An accelerated explicit method with GPU parallel computing for thermal stress and welding deformation of large structure models", *International Journal of Advanced Manufacturing Technology*, 2016.

CONTACT WITH THE AUTHOR

Janusz Kozak
e-mail: kozak@pg.edu.pl

Gdańsk University of Technology
Narutowicza 11/12
80-233 Gdańsk
Poland